Marqueno, T.; Santamaria-Perez, D.; Ruiz-Fuertes, J.; Chulia-Jordan, R.; Jorda Moret, JL.; Rey Garcia, F.; Mcguire, C.... (2018). An Ultrahigh CO2-Loaded Silicalite-1 Zeolite: Structural Stability and Physical Properties at High Pressures and Temperatures. Inorganic Chemistry. 57(11):6447-6455. https://doi.org/10.1021/acs.inorgchem.8b00523

Inorganic Chemistry
Cite This: Inorg. Chem. XXXX, XXX, XXX−XXX
Article
pubs.acs.org/IC

An Ultrahigh CO_2-Loaded Silicalite-1 Zeolite: Structural Stability and Physical Properties at High Pressures and Temperatures

Tomas Marqueño,[†] David Santamaria-Perez,[†,*] Javier Ruiz-Fuertes,[†,‡] Raquel Chuliá-Jordán,[†] Jose L. Jordá,[§] Fernando Rey,[§] Chris McGuire,[∥] Abby Kavner,[∥] Simon MacLeod,[⊥,#] Dominik Daisenberger,[@] Catalin Popescu,[▽] Placida Rodriguez-Hernandez,[○] and Alfonso Muñoz[○]

[†]MALTA-Departamento de Física Aplicada-ICMUV, Universidad de Valencia, E-46100 Valencia, Spain

[‡]MALTA-DCITIMAC, Universidad de Cantabria, E-39005 Santander, Spain

[§]Instituto de Tecnología Química, Universitat Politècnica de València − Consejo Superior de Investigaciones Científicas, E-46022 Valencia, Spain

[∥]Earth, Planetary, and Space Sciences Department, University of California Los Angeles, Los Angeles, California 90095, United States

[⊥]Atomic Weapons Establishment, Aldermaston, Reading RG7 4PR, U.K.

[#]Institute of Shock Physics, Imperial College London, London SW7 2AZ, U.K.

[@]Diamond Light Source, Didcot, Oxon OX11 0DE, U.K.

[▽]CELLS-ARBA Synchrotron, Cerdanyola del Valles, E-08290 Barcelona, Spain

[○]Departamento de Física, Instituto de Materiales y Nanotecnología, MALTA Consolider Team, Universidad de La Laguna, E-38200 La Laguna, Tenerife, Spain

ABSTRACT: We report the formation of an ultrahigh CO_2-loaded pure-SiO_2 silicalite-1 structure at high pressure (0.7 GPa) from the interaction of empty zeolite and fluid CO_2 medium. The CO_2-filled structure was characterized *in situ* by means of synchrotron powder X-ray diffraction. Rietveld refinements and Fourier recycling allowed the location of 16 guest carbon dioxide molecules per unit cell within the straight and sinusoidal channels of the porous framework to be analyzed. The complete filling of pores by CO_2 molecules favors structural stability under compression, avoiding pressure-induced amorphization below 20 GPa, and significantly reduces the compressibility of the system compared to that of the parental empty one. The structure of CO_2-loaded silicalite-1 was also monitored at high pressures and temperatures, and its thermal expansivity was estimated.

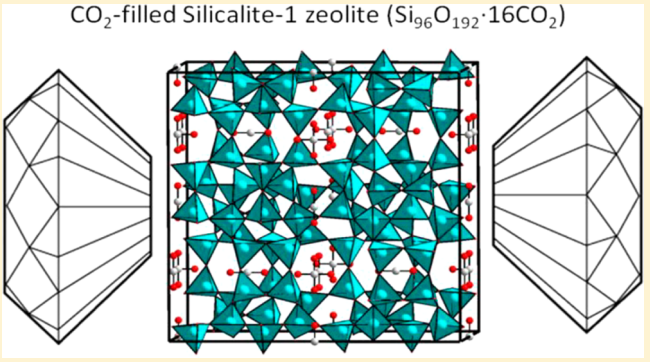

INTRODUCTION

Carbon dioxide (CO_2) is naturally present in the atmosphere as part of the Earth's carbon cycle. It is the primary greenhouse gas emitted through human activities, and its atmospheric concentration has been related to climate change, with a known correlation between periods of high CO_2 concentration and warmer periods.[1] In this context, the scientific community has paid significant attention in the past few years to CO_2 capture and storage in microporous materials.[2,3] Pure silica zeolites have been widely investigated, since they present cages and channel-like voids large enough to accommodate a considerable amount of CO_2 molecules and windows large enough for guest species to pass through.[4,5] Another advantage of these siliceous frameworks is their chemical, thermal, and mechanical stability.

In particular, the MFI-type silicalite-1 zeolite has attracted a lot of interest because of the existence of two different types of channels, straight and sinusoidal, that allow adsorbing aromatics to chain compounds.[6−11] Depending on the nature of the guest molecules, the adsorption process starts in one specific location or the other . Thus, bulky aromatic molecules initially adsorb at the intersection of both channels and then continue in the sinusoidal channel,[6,7] whereas benzene locates at intersections and the straight channel.[8] In the case of non-aromatic hydrocarbons as guest molecules, the molecular configuration determines which channel is the preferred adsorption site. Linear molecules prefer the straight channel, and bent molecules prefer the sinusoidal one.[9] It is worth mentioning that the structural studies on filled silicalite-1 zeolites are difficult since these structures may present twin phases and undergo several phase transitions with varying temperature or mechanical stress.[10] These facts reveal a complex scenario for adsorption in this pure-silica zeolite as well as difficult structural characterization.

Received: February 27, 2018

DOI: 10.1021/acs.inorgchem.8b00523
Inorg. Chem. XXXX, XXX, XXX−XXX

The structures of silicalite-1 with three different concentrations of CO_2 have been recently determined at ambient conditions by means of single-crystal X-ray diffraction (XRD).[2,10,11] "Low-", "mid-", and "high-loaded" CO_2-silicalite-1, obtained by tuning the adsorption time of the zeolite crystals at 0.080 MPa CO_2 gas, were reported to contain 1.5, 4.7, and 5.4 CO_2 molecules per unit cell, respectively. Reported results indicate that the first CO_2 molecules (low-loaded) locate in the straight channel, which is at that time the most stable sorption site. Subsequently, guest molecules start to occupy the sinusoidal pores and intersections (mid- and high-loaded).[2] This behavior was tentatively explained by the role of the van der Waals interactions between carbon dioxide and framework atoms. Results of adsorption isotherms and Monte Carlo simulations show a much higher CO_2 adsorption capacity of about 2.4 mmol/g (~16 molecules/unit cell) at higher pressures of 0.8 MPa, with no significant change above that pressure.[12−15]

An important initial milestone for designing and developing potential long-term CO_2 sequestration strategies is the observation of chemical reactivity between CO_2 and porous silica structures at high pressures (HP) and high temperatures (HT). A silicon carbonate phase was recently synthesized by reacting silicalite and molecular CO_2 which fills the pores in diamond anvil cells (DACs) at 18−26 GPa and 600−980 K.[16] Although the structure of such a compound could not be fully characterized, it was observed to be metastable when temperature quenched. The possibility of carbon dioxide reacting with dense silica and forming a solid solution at similar pressures and higher temperatures (above 1400 K) has, however, been ruled out by direct characterization of the thermodynamically stable phases of CO_2 and SiO_2 at those P−T conditions.[17,18] Therefore, further insights into the chemical and structural stability of CO_2-filled silicalite are needed. The total amount of adsorbed CO_2 molecules in this zeolite at high pressures and temperatures is a key parameter for determining its behavior. It is well-known that the usual compression mechanism in silicalite, which involves the collapse of the structure around the empty pores, is hindered by the presence of the CO_2 guest molecules.[19−21] This leads to the deactivation of the pressure-induced amorphization mechanism observed in the absence of guest species.[20] This effect was also experimentally reported for other CO_2-filled siliceous zeolites, like LTA.[22] Moreover, those experiments, which were performed in DACs using CO_2 as the pressure transmitting medium, also show a concentration of adsorbed carbon dioxide in the LTA zeolite pores (CO_2/SiO_2 = 13/24) at 0.5 GPa[22] that is much larger than the adsorption value (CO_2/SiO_2 = 6−9/24) at 0.5 MPa and 303 K, as calculated from CO_2 adsorption isotherms.[23]

The aim of this work is to better understand the structural behavior of the aforementioned CO_2-filled silicalite-1 compound under compression and heating. The present study allows us to locate the adsorbed CO_2 molecules within the silicalite host framework and to evaluate their mutual chemical interactions. Thus, we report results from angle-dispersive X-ray diffraction experiments up to 20 GPa at room temperature and up to 10 GPa and 750 K. The experiments are complemented with first-principles total-energy calculations, which provide more detailed features of the structure for pressures lower than 4 GPa. Relevant compressibility−expansivity parameters are determined, and structural behavior is discussed.

EXPERIMENTAL DETAILS

The silicalite samples were synthesized using two different methods. (i) The MFI zeolite named silicalite-1-F was prepared according to the IZA recipe[24] with a batch composition of 1 SiO_2/0.08 (TPA)Br/0.04 NH_4F/20 H_2O (175 °C). Pure-silica prismatic crystals of average dimensions 20 × 20 × 40 μm^3 were obtained, which were subsequently crushed in a mortar with a pestle for high-pressure experiments. (ii) The MFI zeolite named silicalite-1-OH was prepared according to ref 25 with a batch composition of 1 SiO_2/9.7 EtOH/0.25 TPAOH/24 H_2O (150 °C). The sample obtained using this method is polycrystalline. These two silicalite compounds slightly differ in composition, with the latter having more Si vacancies (approximately 3% OH groups were reported[25]), but both structures have the same crystal symmetry (S.G. $P2_1/n$, as we will see in the Results and Discussion). In other words, the existence of the OH groups in silicalite-1-OH entails scarce interruptions of the tetrahedral framework due to the fact that those OH apexes are not shared with adjacent tetrahedra. The samples were characterized at room conditions using a Bruker D8 Advance A25 diffractometer with a Cu Kα (λ = 1.5406 Å) tube and a Linx Eye detector.

Two different kinds of high-pressure experiments were performed, one at room temperature (RT) and the other at high temperature (HT, up to ~750 K). For the HP−RT condition experiments, both types of silicalite samples were placed inside different symmetric diamond anvil cells and characterized *in situ*. For the silicalite-1-F sample, the DAC was equipped with 300 μm culet diamonds; the rhenium gasket was pre-indented to a thickness of 35 μm, and a pressure chamber of 100 μm diameter was prepared. In the silicalite-1-OH case, the diamonds had 500 μm culets, and the rhenium gasket was pre-indented to a thickness of 42 μm. The hole in which the sample was placed had a diameter of 200 μm. In both cases, the silicalite sample was placed together with some Pt metal, in order to use its equation of state (EoS) as an internal pressure gauge.[26] Besides the sample and Pt metal, the DAC was loaded with high-purity CO_2 at room temperature using a COMPRES gas loading machine. The CO_2 is expected to work as a pressure transmitting medium and diffuse into the zeolite channels. Pressures derived from the CO_2−I phase EoS[27,28] are consistent with those obtained from Pt. We carried out *in situ* HP−RT angle-dispersive XRD measurements at a synchrotron-based GSECARS beamline at the Advanced Photon Source. The X-ray wavelength was 0.4592 Å, and the beam was focused to a ~5 × 5 μm^2 spot. XRD patterns were obtained using a CCD camera with time lapses of 5−40 s.

For the HP−HT measurements, a gas-driven membrane DAC with 350 μm culet diamonds was used. This DAC was loaded with the silicalite-1-F sample in a pressure chamber of similar dimensions as that previously described. The CO_2 was loaded inside the DAC at room temperature using the Sanchez Technologies loading machine available in the Diamond Light Source synchrotron facility. Instead of Pt metal, in this case we used NaCl powder as a pressure standard.[29] The DAC was heated using a resistive heating device known as Watlow 240V (rated at 4.65 W cm^{-2}), which consists of a coiled heater wrapped around the DAC. Temperature was measured using a K-type thermocouple placed near the gasket. This thermocouple provides temperature measurements to 0.4% precision in the range covered by our experiment. In order to avoid diamond graphitization, the DAC was placed inside a custom-built vacuum vessel specially designed for HP−HT experiments.[22] The XRD measurements were performed in the MSPD beamline in the ALBA-CELLS synchrotron[30] using a wavelength of 0.534 Å. The X-ray beam was focused to ~20 × 20 μm^2 by using Kirkpatrick−Baez mirrors, and the diffraction patterns were collected by a Rayonix CCD detector.

LaB_6 and CeO_2 powders were used as calibrants, and the integration of the XRD patterns from raw to conventional 2θ intensity data was carried out with Dioptas software.[31] The indexing and refinement of the XRD patterns were performed using the PowderCell[32,33] and UnitCell[34] program packages. The diffraction contribution of the kapton windows of the vacuum vessel (empty cell in the vessel) was subtracted in HP−HT XRD experiments.[35]

DOI: 10.1021/acs.inorgchem.8b00523
Inorg. Chem. XXXX, XXX, XXX−XXX

THEORETICAL DETAILS

Zeolite modeling was carried out through ab initio total-energy simulations using the density functional theory (DFT)[36] with the Vienna Ab Initio Simulation Package (VASP).[37−39] The projector-augmented wave (PAW)[40] scheme was adopted as it reproduces the full nodal character of the wave function in the core region. The basis set of plane waves was extended up to a large energy cutoff of 520 eV, due to the presence of oxygen. To take into account the exchange correlation energy, we used the generalized gradient approximation (GGA) in the form of Perdew−Burke−Ernzerhof for solids (PBEsol).[41] We also performed simulations including van der Waals (vdW) corrections with a PBE[42] functional for the exchange correlation energy and the Grime D2[43,44] method to include long-range dispersion corrections, as implemented in the VASP package. Due to the large size of the cell with a great number of atoms (336), we used only the Γ k-point to perform integrations over the Brillouin zone (BZ). In order to determine the ground state properties and theoretical optimized structure, we had to relax the structure with a high number of degrees of freedom. The convergence in total energy was considered achieved when the difference between two consecutive iterations was less than 10^{-5} eV/atom. In the theoretically optimized structures at different volumes, the maximum of the Hellmann−Feynman forces on each atom was 0.01 eV/Å and the deviation of the stress tensor from a diagonal hydrostatic form was about 0.1 GPa. For several different volumes, the structure was optimized to obtain a set of energies (E) and pressures (P) for each case considered.

RESULTS AND DISCUSSION

Figure 1 shows the XRD pattern of empty silicalite-1-OH at room conditions (λ_{Cu} = 1.5406 Å). A Rietveld refinement gave

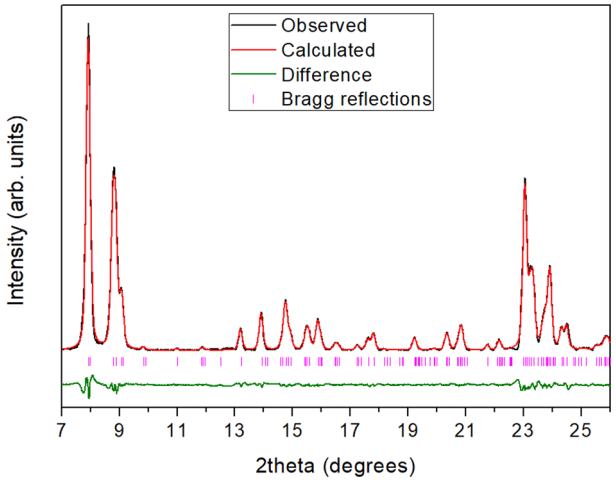

Figure 1. Rietveld refinement of the XRD pattern of the silicalite-1-OH sample at room conditions (λ_{Cu} = 1.5406 Å). The observed, calculated, and difference patterns are represented as black, red, and green lines, respectively. Vertical magenta lines indicate Bragg reflections.

lattice parameters and atomic coordinates similar to those previously reported:[45,46] monoclinic space group (S.G.) $P2_1/n$, a = 19.9057(3) Å, b = 20.1144(3) Å, c = 13.3918(2) Å, β = 90.47(1)°, and V = 5361.8(6) Å^3, for 96 formula units per cell. About 3% of the O positions were substituted by OH groups in the model used for the refinement, as previously suggested in the literature.[46] The XRD pattern of the silicalite-1-F sample was indexed with the same monoclinic space group and lattice parameters of a = 19.9352(3) Å, b = 20.1775(4) Å, c = 13.4286(2) Å, β = 90.81(1)°, and V = 5401.0(7) Å^3.

After CO_2-gas loading and compression to 0.7 GPa, the XRD pattern of silicalite-1-OH changes significantly. Figure 2a shows

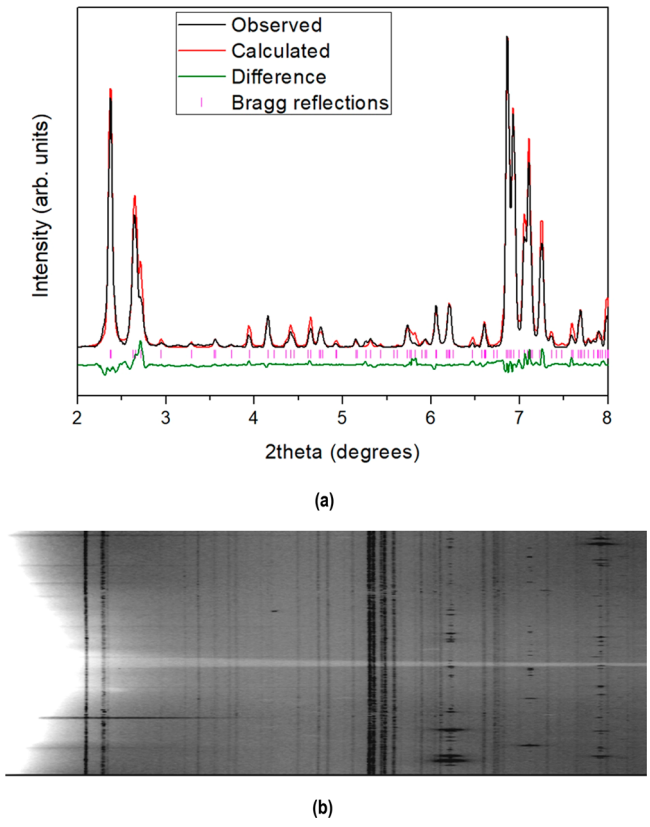

Figure 2. (a) Rietveld refinement of the XRD pattern of the silicalite-1-OH sample at 0.7 GPa and room temperature (λ = 0.4592 Å). The observed, calculated, and difference patterns are represented as black, red, and green lines, respectively. Vertical magenta lines indicate Bragg reflections. (b) Unrolled (or cake) image of the raw data from the CCD detector at these pressure and temperature conditions to illustrate the quality of our data.

the integrated XRD pattern at that pressure (λ = 0.4592 Å). In particular, when comparing the normalized XRD patterns of the CO_2-filled (Figure 2a) and the empty silicalite (Figure 1) structures, we realized that the intensity of the group of peaks placed between 1.6 and 1.766 d-spacings (2θ = 22.6−25° in Figure 1, and 2θ = 6.7−7.4° in Figure 2a) is approximately 2 times higher in the case of the CO_2-filled structure. The excellent quality of the XRD data, illustrated in Figure 2b with the caked image of the raw CCD image, encourages us to fully characterize the structure of the CO_2-filled zeolite. Thus, at 0.7 GPa, the zeolite structure can be described as an orthorhombic *Pnma* (S.G. no. 62) MFI-type phase, similar to that initially reported in the literature for "high-loaded" CO_2-silicalite,[11] with comparable lattice parameters: a = 20.021(2) Å, b = 19.818(8) Å, c = 13.361(6) Å, and V = 5301(5) Å^3 (Table 1).

The large pores associated with the sinusoidal and straight channels, with diameters of approximately 4.6 Å,[47] give silicalite-1 its properties of being a good adsorbent. The locations of the guest carbon dioxide molecules were found by Rietveld refinement and difference-Fourier maps of the electron density function,[22,48] assuming that the atomic coordinates of the host framework have not changed significantly between the empty structure at ambient pressure and the CO_2-filled structure at 0.7 GPa. Thus, the electron density maps obtained

DOI: 10.1021/acs.inorgchem.8b00523
Inorg. Chem. XXXX, XXX, XXX−XXX

Table 1. Powder Diffraction Data of CO_2-Loaded Silicalite at 0.7 GPa Pressure and Room Temperature

source: synchrotron
chemical formula: $C_{16}Si_{96}O_{224}$ (16 CO_2·96 SiO_2)
formula weight: 6472.11
temperature: 298 K
pressure: 0.7 GPa
wavelength: 0.4592 Å
crystal system: *Pnma*
space group (no.): 62
a = 20.021(2) Å, b = 19.818(8) Å, c = 13.361(6) Å, α = 90°, β = 90°, γ = 90°
V = 5301(5) Å^3
d-space range: 2.78−26.00
χ^2 = 12.05
R_p = 23.1
R_{wp} = 41.2

from Fourier difference sections derived from the contributions of the [SiO_4] units of the silicalite framework allowed us to locate the CO_2 molecules in the porous structure. Figure 3, for

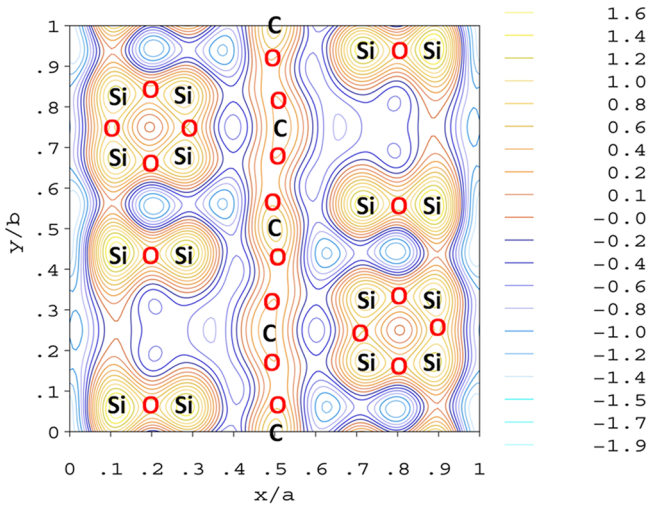

Figure 3. Bidimensional Fourier map of the plane z = 0 in CO_2-filled silicalite calculated using X-ray structure factors.

instance, clearly shows the existence of residual density maxima along the straight channels in plane z = 0. Further Fourier maps were then computed, and they reveal additional sites for carbon dioxide centered in the sinusoidal channels. The known dimensions of the CO_2 molecule (C−O distances of 1.17 Å) and the room availability in the channels also helped to constrain the adsorption capacity by delimiting the interatomic distance cutoffs. The atomic coordinates of the C and O atoms so determined, together with the positions of the Si and O atoms of the host framework, are collected and reported in a cif file noted with the Accession Codes. Figure 4 shows the structure of this CO_2-filled silicate-1 compound. The insertion of 16 CO_2 molecules per unit cell into the refinement causes a considerable improvement to the fit, according to visual judgment (Figure 2a, R_p = 15.6 and R_{wp} = 34.4), evincing the existence of an ultrahigh CO_2-loaded silicalite-1 zeolite at 0.7 GPa.

Note that this adsorption value at RT (16 CO_2 molecules/unit cell) is much larger than that of the silicalite-1 zeolite at lower pressures of 0.08 MPa (5.4 CO_2 molecules/unit cell) and 298 K, as determined from single-crystal X-ray diffraction.[11] In

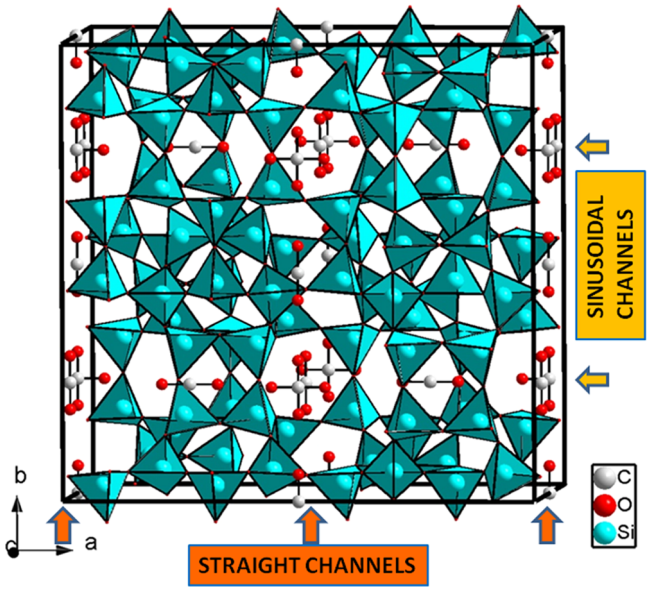

Figure 4. View of the CO_2-filled silicalite structure along the c axis showing both the host silicalite framework structure and the location of CO_2 molecules at 0.7 GPa. Gray, cyan, and red spheres represent Si, C, and O atoms, respectively.

the same manner as this previously reported "high-loaded" CO_2 silicalite, the adsorption content of our CO_2-filled structure is in perfect agreement with the extrapolation of the adsorption isotherm curves at 303 K existing in the literature,[13,14] with 16 adsorvated CO_2 molecules for P > 1 MPa. Previous studies stated that increasing pressure over the 0.5 MPa range had no significant effect on CO_2 adsorption capacity, which is consistent with the experimental observation that peak intensity ratios in XRD patterns are stable at higher pressures, as can be seen in Figure 5.

Figure 5 shows the XRD patterns of CO_2-filled silicalite up to 13.2 GPa. At first glance, no direct evidence of structural phase transition, such as appearance or disappearance of diffraction peaks, was observed. The observation of low-2θ-angle X-ray diffraction lines even at the highest pressure provides evidence of the absence of pressure-induced amorphization (PIA), as a consequence of complete filling of the pores by CO_2.[20] The initial phase seems to be stable up to the maximum pressure reached in the present study, although the bad quality of the patterns at the highest pressures and the complex structure preclude an unequivocal indexing. Nevertheless, the indexing of the lower-pressure XRD patterns reveals that the difference in length between the a and b axes decreases with increasing pressure and the values converge at a pressure of about 4 GPa (see Tables 2 and 3 and Figure 6). From that pressure, the experimental XRD patterns could be explained with a pseudotetragonal phase (a = b), in good agreement with previous results reported in the literature.[21] Thus, there are two different axial compressibility regimes for the CO_2-filled silicalite-1-OH (silicalite-1-F): (i) for P < 4 GPa, where $\beta_a \sim 1.3(1.2)\beta_b \sim 1.6(1.4)\beta_c$, and (ii) for P > 4 GPa, where $\beta_{b,a} \sim 1.3(1.2)\beta_c$. The axial compressibility values are collected in Tables 4 and 5 and define the slight anisotropy of this material. As can be seen in Figure 7, our P−V data are in good agreement with those existing in the literature and show the absence of volume discontinuity in the studied pressure range. The fit of our P−V silicalite-1-OH data together with those of

DOI: 10.1021/acs.inorgchem.8b00523
Inorg. Chem. XXXX, XXX, XXX−XXX

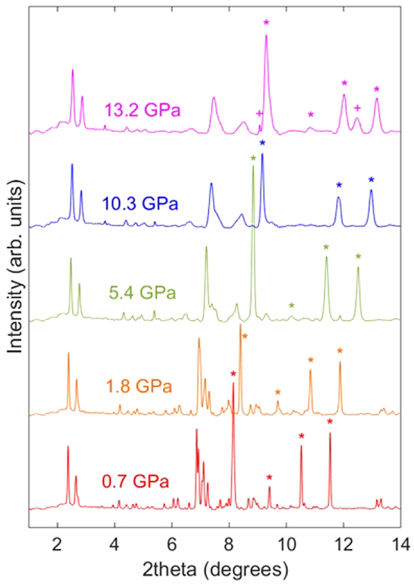

Figure 5. Selected powder XRD patterns of CO_2-filled silicalite-1-OH zeolite up to 13.2 GPa (λ = 0.4592 Å). CO_2–I and CO_2–III peaks are indicated by "*" and "+", respectively. Low-angle Bragg peaks (2θ < 4°) keep their width and relative intensity in this pressure range. As pressure increases, some peaks start to combine together until ∼5 GPa, as the structure goes from orthorhombic to tetragonal. For higher pressures and 2θ > 4°, the silicalite peaks broaden and their intensities decrease. This may suggest a pressure-induced loss of crystallinity.

Table 2. Unit Cell Parameters of Silicalite-1-OH with Pressure (HP–RT Data)

P (GPa)	a (Å)	b (Å)	c (Å)	V (Å^3)
0.7	20.0212(17)	19.818(8)	13.361(6)	5301(5)
0.7	20.0208(11)	19.814(2)	13.358(2)	5299(2)
0.7	20.0222(9)	19.810(3)	13.356(3)	5299(2)
1.0	19.9533(9)	19.7601(7)	13.3354(14)	5257(1)
1.0	19.9534(7)	19.7525(14)	13.3284(15)	5253(1)
1.8	19.7974(9)	19.6438(14)	13.272(2)	5161(2)
1.8	19.7920(7)	19.6481(8)	13.2741(3)	5161(2)
2.6	19.594(3)	19.486(2)	13.178(4)	5031(3)
2.7	19.595(2)	19.4711(15)	13.172(1)	5026(2)
4.0	19.2641(14)	19.2641(14)	12.996(5)	4823(7)
4.2	19.239(8)	19.239(8)	12.990(6)	4808(4)
5.4	19.051(7)	19.051(7)	12.885(6)	4677(4)
5.6	19.047(7)	19.047(7)	12.913(7)	4685(3)
7.7	18.821(11)	18.821(11)	12.781(9)	4528(5)
8.4	18.719(8)	18.7189(8)	12.6940(8)	4448(4)
10. 0	18.565(11)	18.565(11)	12.67(1)	4366(5)
11.0	18.48(1)	18.48(1)	12.594(8)	4299(5)
13.2	18.41(2)	18.42(2)	12.59(2)	4265(16)
13.8	18.32(3)	18.32(3)	12.51(1)	4215(17)

Sartbaeva and co-workers[21] to a third-order Birch–Murnaghan equation of state[49] yields a zero-pressure volume V_0 = 5433(58) Å^3, a bulk modulus B_0 = 26(4) GPa, and a bulk modulus pressure derivative B'_0 = 5.5(7). Silicalite-1-F pressure–volume data slightly deviate from those of silicalite-1-OH above 5 GPa, so we fitted them with a third-order Birch–Murnaghan EoS, fixing B'_0 to 5.5, obtaining as characteristic parameters V_0 = 5499(32) Å^3 and B_0 = 21(1) GPa. All the experimental and theoretical EoS parameters for silicalite-1 samples are collected

Table 3. Unit Cell Parameters of Silicalite-1-F with Pressure (HP–RT Data)

P (GPa)	a (Å)	b (Å)	c (Å)	V (Å^3)
0.7	20.019(4)	19.8107(103)	13.355(7)	5296(7)
2.0	19.7121(14)	19.598(3)	13.235(3)	5113(3)
2.0	19.777(3)	19.634(5)	13.233(2)	5140(3)
2.8	19.551(4)	19.453(4)	13.093(6)	4980(4)
2.8	19.5718(19)	19.4691(17)	13.109(2)	4995(2)
4.8	19.088(14)	19.088(14)	12.876(9)	4692(7)
6.9	18.827(15)	18.827(15)	12.699(15)	4501(12)
9.4	18.59(2)	18.59(2)	12.561(15)	4340(16)
15.0	18.07(3)	18.07(3)	12.41(2)	4052(20)

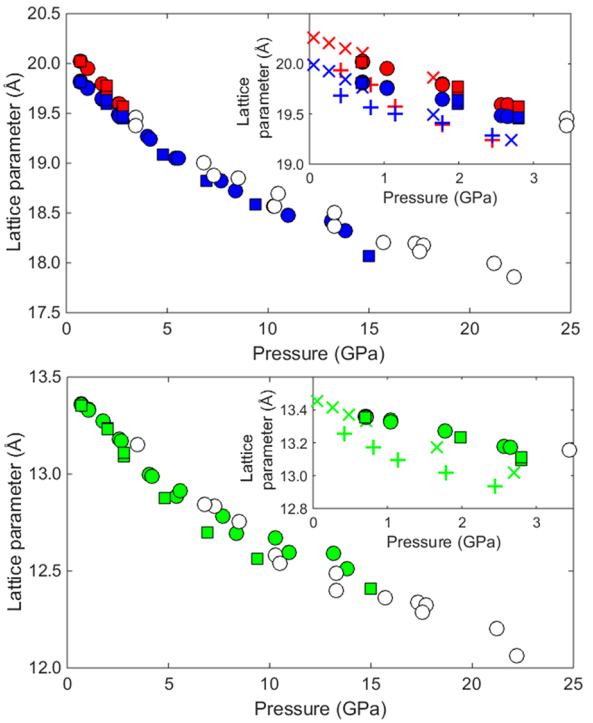

Figure 6. Lattice parameters of silicalite-OH (circles) and silicalite-1-F (squares). Open symbols represent the reported data by Sartbaeva and co-workers,[21] while filled symbols represent ours. The top figure shows the a and b lattice parameters, indicated in red and blue, respectively. In the bottom figure, the evolution of the c parameter is displayed (green symbols for our data). The refinement was carried out using PowderCell in the orthorhombic range. Once the a and b lattice parameters converged, as it is shown, it was possible to use both PowderCell and UnitCell software packages, since there were more isolated peaks. Insets: Enlargement of the lattice parameters vs pressure graphs in the 0 < P < 3.5 GPa range, including the results from PBEsol (× symbols) and PBE+VdW (+ symbols) theoretical calculations.

in Table 6. It is worth noting that the unit cell volume of the zeolite has increased about 1.4% with CO_2 adsorption, as inferred from the RP–RT unit cell volume data of the empty zeolite and the zero-pressure volume estimated from the RT CO_2-filled zeolite EoS. CO_2-filled silicalite is approximately three times less compressible than the parental empty system in response to the pore-filling effect. The bulk modulus obtained in the present work is slightly smaller than that found for silicalite-1 filled with other atoms or molecules like Ar (B_0 = 35.9 GPa)[19] or ammonia borane (B_0 = 39.1 GPa).[50] Moreover, its compressibility behavior is comparable to that of other CO_2-

DOI: 10.1021/acs.inorgchem.8b00523
Inorg. Chem. XXXX, XXX, XXX–XXX

Table 4. Extrapolated Lattice Parameters of CO_2-Filled Silicalite at Room Conditions and Axial Compressibilities for Pressures Lower Than 4 GPa

	silicalite-1-OH	silicalite-1-F	PBEsol calculations	PBE+VdW calculations
a_0 (Å)	20.193(8)	20.22(6)	20.271	20.064
β_a (GPa^{-1})	0.0111(5)	0.011(3)	0.014	0.018
b_0 (Å)	19.952(16)	20.01(5)	20.017	19.792
β_b (GPa^{-1})	0.0087(6)	0.009(2)	0.015	0.011
c_0 (Å)	13.456(18)	13.48(3)	13.465	13.341
β_c (GPa^{-1})	0.0070(7)	0.008(3)	0.013	0.012

Table 5. Extrapolated Lattice Parameters of CO_2-Filled Silicalite at Room Conditions and Axial Compressibilities for Pressures Higher Than 4 GPa

	silicalite-1-OH	silicalite-1-F
a_0 (Å)	19.988(13)	19.92(5)
β_a (GPa^{-1})	0.0063(4)	0.006(5)
c_0 (Å)	13.39(4)	13.24(9)
β_c (GPa^{-1})	0.0049(7)	0.005(2)

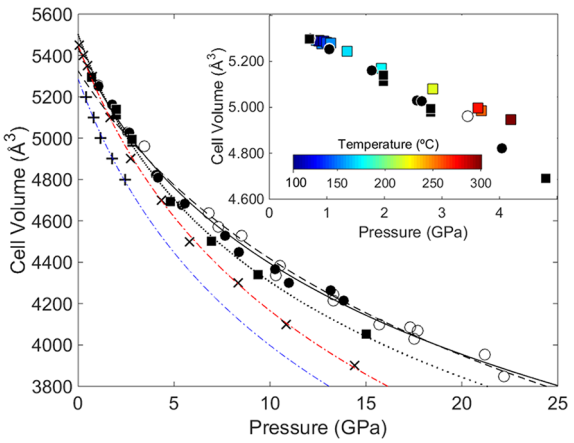

Figure 7. Cell volume vs pressure for silicalite-1-OH (circles) and silicalite-1-F (squares) with CO_2. Solid and empty symbols stand for the experimental data from our present study and the study by Sartbaeva and co-workers,[21] respectively. The dashed line represents the least-squares fit to the literature experimental data with a second-order Birch–Murnaghan fit (V_0 = 5325 Å^3, B_0 = 36.8 GPa). The solid line is the third-order Birch–Murnaghan EoS fit to the combined data sets of our silicalite-1-OH and that of Sartbaeva and co-workers,[21] which gives V_0 = 5438 Å^3, B_0 = 26.0 GPa, and B'_0 = 5.55. The dotted line stands for a second-order Birch–Murnaghan EoS fit to our silicalite-1-F data, which yields V_0 = 5501 Å^3 and B_0 = 20.7 GPa by setting B'_0 = 5.55. Results from PBEsol (× symbols) and PBE+VdW (+ symbols) theoretical calculations are also shown. Inset: Colored squares are the silicalite-1-F HP–HT data. The temperature range covered in the experiment is displayed in the color bar. Blue and red dash–dot lines are fits to the calculation data.

filled pure-silica zeolites. The bulk modulus of the filled ITQ-29 LTA zeolite, for instance, was experimentally determined to be 38 GPa,[22] whereas the bulk modulus of the filled RHO-type zeolite was theoretically estimated to be 27 GPa,[51] after fitting the P–V data with a second-order Birch–Murnaghan EoS. It is also worth noting that the complete filling of the pores by CO_2 in an equilibrium process with the rest of CO_2 outside the

Table 6. Experimental and Theoretical CO_2-Filled Silicalite-1 EoS Parameters

	silicalite-1-OH	silicalite-1-F	PBEsol calculations	PBE+VdW calculations
V_0 (Å^3)	5433(58)	5499(32)	5469(5)	5286(14)
B_0 (GPa)	26(4)	21(1)	20.1(4)	20.4(9)
B'_0	5.5(7)	5.5(fixed)	4(fixed)	4(fixed)

pores that acts as pressure transmitting medium confers to the zeolite a compressibility lower than or comparable to those of some low-pressure silica polymorphs, i.e., low-cristobalite and low-quartz have bulk moduli of 16 and 38 GPa, respectively.[52]

Total-energy calculations at 0 K were performed using the orthorhombic structural model inferred from XRD measurements. Two different approximations were considered: PBEsol and PBE+VdW, as explained in the Theoretical Details. As simulations cannot cope with non-integer occupational factors, we relaxed two different structural types that differ only in the orientation of the CO_2 molecules located at the channel intersections. In case 1, the CO_2 molecules are oriented parallel to the a axis and the sinusoidal channels, whereas in case 2, they are parallel to the b axis and the straight channels. The difference in energy between the two different relaxed structures is less than 95 meV per unit cell (note that there are 336 atoms in the cell). In both cases, the theoretically optimized structure does not differ much from that inferred from XRD measurements, as can be inferred from the cif files noted in the Accession Codes, with only a slight tilting of certain CO_2 molecules located in the straight channels. The XRD patterns simulated using the relaxed structures as models do not improve the Rietveld fit to the experimental data. In terms of unit cell volume evolution with increasing pressure, the better agreement is obtained with the PBEsol prescription, which is found to reproduce with less than 1% uncertainty the volume of CO_2-filled SiO_2 silicalite obtained experimentally below 3.5 GPa. Figure 7 shows the theoretical unit cell volume results with both approximations, compared to the experimental behavior. It can be observed that the PBE+VdW prescription underestimates the unit cell volume by 4%. Thus, second-order Birch–Murnaghan EoS fits of our *ab initio* PBEsol and PBE+VdW results yield zero-pressure volumes, V_0, of 5469(5) and 5286(14) Å^3 and bulk moduli, B_0, of 20.1(4) and 20.4(9) GPa, respectively (see Table 6 for the sake of comparison with experimental data). Regarding the pressure dependence of the lattice parameters, our calculations using PBEsol prescription do not reproduce the convergence of the a and b axes observed experimentally, but those using PBE+VdW do, at a lower pressure (2 GPa). However, as opposed to the experimental observations, our PBE+VdW simulations reveal that this point is just an intersection of the a and b axial lengths, as $b > a$ for $P > 2$ GPa. In other words, the linear axial compressibilities can be described by a unique regime where $\beta_a \sim 1.6\beta_b \sim 1.5\beta_c$. For unit cell volumes smaller than 4600 Å^3 ($P > 4$ GPa), the relaxation of the forces on the atoms was very difficult to achieve for the PBE+VdW simulations, even using greater Monkhorst–Pack meshes for the integrations over the BZ, so we perform simulations only up to 4 GPa. Moreover, PBE+VdW theoretical calculations predict a small triclinic distortion above that pressure, with angles very close to 90°. However, the simulations using the PBEsol prescription for the exchange correlation energy do not reproduce this triclinic distortion; indeed, the structure is predicted to remain

DOI: 10.1021/acs.inorgchem.8b00523
Inorg. Chem. XXXX, XXX, XXX–XXX

Table 7. Unit Cell Parameters of Silicalite-1-F at High Pressures and High Temperatures (HP−HT Data)

P (GPa)	T (°C)	a (Å)	b (Å)	c (Å)	V (Å^3)
1.1	104	19.9911(15)	19.834(3)	13.339(3)	5289(2)
1.2	122	19.986(3)	19.8251(12)	13.344(4)	5288(3)
1.2	138	19.9884(11)	19.8213(9)	13.337(4)	5283(2)
1.3	156	19.976(1)	19.8166(15)	13.3360(17)	5279(2)
1.6	170	19.9177(13)	19.767(2)	13.3165(9)	5243(2)
2.1	176	19.787(11)	19.674(16)	13.270(7)	5170(10)
3.0	220	19.665(5)	19.571(5)	13.204(3)	5081(4)
3.9	255	19.547(3)	19.427(3)	13.132(6)	4986(4)
3.8	271	19.55(2)	19.45(3)	13.139(8)	4997(16)
4.4	301	19.45(2)	19.375(15)	13.125(17)	4946(15)

orthorhombic to 28 GPa, where the structure becomes monoclinic. Our theoretical data up to 4 GPa also show us that the mechanism of structural deformation of the zeolitic framework under compression is the increase of channel ellipticity. Thus, using flattering $f = (D - d)/D$ as a mesure of the compression of the pores of the straight channel along its diameter, we can see that this f parameter drastically increases from 0.096 at room pressure to 0.192 at 1.1 GPa (see cif files from theoretical simulations via the Accession Codes).

Besides the room temperature compression experiments, we also carried out high-pressure−high-temperature XRD measurements in order to get further insight into the phase diagram of this CO_2/SiO_2 binary system and to estimate, if possible, the thermal expansivity of the CO_2-filled silicalite. We progressively compress and heat the CO_2-filled silicalite-1-F sample to 10 GPa and 700 K. This run allowed us to determine that the initial silicalite structure at 3.6 GPa remains stable up to 536 K, with a temperature only slightly higher than the melting temperature of the CO_2 pressure transmitting medium at that pressure (522 K), where it decomposed into the thermodynamically stable phases of carbon dioxide and silica at those conditions: CO_2 melt and quartz.[53] The indexed lattice parameters of the CO_2-filled silicalite-1-F at different pressure and temperature conditions are collected in Table 7, and the unit cell volumes are depicted in the inset of Figure 7. Further heating to 700 K and compression entail the transformation of silica into the coesite phase at 5 GPa, in good agreement with previous delimitations of the quartz−coesite phase boundary.[54] In addition to that, our $P-V-T$ data were used to roughly estimate the linear thermal expansivity of CO_2-filled silicalite-1-F at ∼1.2 GPa in the temperature range between 293 and 450 K as approximately $1.0(5) \times 10^{-4}$ K^{-1}. Another estimation of the thermal expansivity is obtained using all our $P-V-T$ data and a first order Taylor expansion of volume in terms of pressure and temperature, where the reference volume is subtracted at each pressure and then normalized.[22] This method gives a thermal expansivity value of $1.5(3) \times 10^{-4}$ K^{-1} between 1 and 4.5 GPa and 293 and 530 K. These values are higher than that obtained for CO_2-filled pure-silica LTA zeolite ($6.6(2) \times 10^{-5}$ K^{-1}).[22]

CONCLUDING REMARKS

Penetrability of external molecules in zeolites at high pressure is known to be governed by several variables; among those, the most important variables are the diameter of the cavities, the pressure of the penetrating molecular fluid, the temperature at which the experiment is conducted, and the chemical nature and configuration of the extra-framework population.[55−57] Pure silica zeolitic frameworks like silicalite-1-F avoid the latter of these variables and give us the opportunity to examine the effect of pressure and temperature without the interference of charge-balancing cations. This study provides the structural characterization of the CO_2-filled silicalite-1 zeolite at full adsorption capacity and equilibrium conditions. XRD characterization shows the adsorption of 16 CO_2 molecules per unit cell and the preferred (most stable) sorption sites, completing the overview of the adsorption process in this porous silica material.[2,10,11] The van der Waals interactions between the CO_2 molecules and the atoms of the silicate groups of the host framework make the former prefer the channels rather than the larger cavities at the intersections. At the high pressures reported here, the CO_2 molecules occupy as much space within the pores as possible and the interactions between them become significant. The compressibility behavior of the filled structure, which is similar to that of most compact silica polymorphs, confirms this point and indicates direct compression of the framework. According to calculations, tilting of the [SiO_4] tetrahedra is the dominant compression mechanism and produces the ellipsoidal deformation of the channels.

The CO_2 adsorption capacity of this silica zeolite at maximum loading (CO_2/SiO_2 = 1/6) is significantly smaller than that of other zeolites with larger pores and cavities, such as the LTA and RHO types, which accommodate 13/24[22] and 1/1[51] molecules of CO_2 per SiO_2 molecule, respectively. However, the CO_2 molecules in silicalite-1 are closer to the silica framework, and this could favor chemical interactions between host and guest species. Thus, the location of the carbon dioxide molecules defines the interatomic distance between the C atom of carbon dioxide and the nearest O atoms of the host silica framework. According to our theoretical calculations at room pressure, this distance is 3.10 Å (compared to the intramolecular C−O distance, 1.17 Å). The shortest distance between Si atoms and O atoms of the CO_2 molecule, on the other hand, is approximately 3.35 Å. According to simulations using the 1:1 stoichiometric ratio[51] in a RHO-type zeolite, a phase transition giving rise to a carbonate structure would occur when the $C_{CO_2}-O_{SiO_2}$ and $Si-O_{CO_2}$ distances are on the order of 2.3 and 2.55 Å, respectively.[51] Taking into account the rapid decrease of these two sets of distances with increasing pressure in CO_2-filled silicalite, we expect that this silicate−carbonate formation should occur at pressures of about 26 GPa. This fact seems to be confirmed by a recent study on this system which reported the formation of a silicate−carbonate phase at pressures of 19−27 GPa and temperatures of 700−900 K.[16] Therefore, these results, together with the scarce literature data on CO_2-adsorbed pure-silica zeolite

DOI: 10.1021/acs.inorgchem.8b00523
Inorg. Chem. XXXX, XXX, XXX−XXX

systems, could allow progression in the design of potential long-term CO_2 sequestration strategies.

■ ASSOCIATED CONTENT

Accession Codes

CCDC 1827571, 1827575, 1827582, and 1827597 contain the supplementary crystallographic data for this paper. These data can be obtained free of charge via www.ccdc.cam.ac.uk/data_request/cif, or by emailing data_request@ccdc.cam.ac.uk, or by contacting The Cambridge Crystallographic Data Centre, 12 Union Road, Cambridge CB2 1EZ, UK; fax: +44 1223 336033. The cif files correspond to the experimental refinement of CO_2-filled silicalite-1-OH at 0.7 GPa and ambient temperature; theoretical structure of CO_2-filled silicalite-1 at 0.05 GPa calculated within the PBEsol prescription, theoretical structure of CO_2-filled silicalite-1 at 0 GPa calculated within the PBE prescription and VdW corrections; and theoretical structure of CO_2-filled silicalite-1 at 1.1 GPa calculated within the PBE prescription and VdW corrections.

■ AUTHOR INFORMATION

Corresponding Author

*E-mail: dsantamaria@quim.ucm.es.

ORCID

David Santamaria-Perez: 0000-0002-1119-5056
Jose L. Jordá: 0000-0002-0304-5680
Alfonso Muñoz: 0000-0003-3347-6518

Notes

The authors declare no competing financial interest.

■ ACKNOWLEDGMENTS

The authors thank the Spanish Ministerio de Economıa y Competitividad (MINECO), the Spanish Research Agency (AEI), and the European Fund for Regional Development (FEDER) for their financial support (MAT2016-75586-C4-1-P, MAT2016-75586-C4-3-P, MAT2015-71842-P; Severo Ochoa SEV-2012-0267; and MAT2015-71070-REDC (MALTA Consolider)). D.S.-P. and J.R.-F. acknowledge MINECO for a Ramón y Cajal (RyC-2014-15643) and a Juan de la Cierva (IJCI-2014-20513) contract, respectively. A.K. acknowledges the support of the University of Valencia through the Grant UV-INV-EPC17-548561. Portions of this work were performed at GeoSoilEnviroCARS (Sector 13), Advanced Photon Source (APS), and Argonne National Laboratory. GeoSoilEnviroCARS is supported by the National Science Foundation, Earth Sciences (EAR-1128799), and the Department of Energy, GeoSciences (DE-FG02-94ER14466). This research used resources from the Advanced Photon Source, a U.S. Department of Energy (DOE) Office of Science User Facility operated for the DOE Office of Science by Argonne National Laboratory (DE-AC02-06CH11357). Use of the COMPRES-GSECARS gas loading system was supported by COMPRES under NSF Cooperative Agreement EAR 11-57758. CO_2 gas was also loaded at Diamond Light Source. The authors thank the synchrotron facility ALBA-CELLS for beamtime allocation at MSPD line.

■ REFERENCES

(1) http://www.epa.gov/climatechange/ghgemissions/gases/co2.html.

(2) Fujiyama, S.; Kamiya, N.; Nishi, K.; Yokomori, Y. Adsorption process of CO2 on silicalite-1 zeolite using single-crystal x-ray method. *Langmuir* **2014**, *30*, 3749−3753.

(3) Guo, P.; Shin, J.; Greenaway, A. G.; Min, J. G.; Choi, H. J.; Liu, L.; Cox, P. A.; Hong, S. B.; Wright, P. A.; Zou, X.; Su, J. A zeolite family with expanding structural complexity and embedded isoreticular structures. *Nature* **2015**, *524*, 74−78.

(4) Liebau, F. *Structural Chemistry of Silicates. Structure, Bonding and Classification*; Springer Verlag: Berlin, Germany, 1985.

(5) Santamaria-Perez, D.; Liebau, F. Structural relationships between intermetallic clathrates, porous tectosilicates and clathrate hidrates. *Struct. Bonding (Berlin, Ger.)* **2010**, *138*, 1−29.

(6) van Koningsveld, H.; Jansen, J. C. Single crystal structure analysis of zeolite H-ZSM-5 loaded with naphtalene. *Microporous Mater.* **1996**, *6*, 159−167.

(7) Nishi, K.; Hidaka, A.; Yokomori, Y. Structure of toluene6.4-ZSM-5 and the toluene disproportionatuon reaction on ZSM-5. *Acta Crystallogr., Sect. B: Struct. Sci.* **2005**, *61*, 160−163.

(8) Kamiya, N.; Iwama, W.; Kudo, T.; Nasuno, T.; Fujiyama, S.; Nishi, K.; Yokomori, Y. Determining the structure of the benzene7.2-silicalite-1 zeolite using a single crystal x-ray method. *Acta Crystallogr., Sect. B: Struct. Sci.* **2011**, *67*, 508−515.

(9) Fujiyama, S.; Seino, S.; Kamiya, N.; Nishi, K.; Yoza, K.; Yokomori, Y. Adsorption structures of non-aromatic hydrocarbons on silicalite-1 using the single-crystal X-ray diffraction method. *Phys. Chem. Chem. Phys.* **2014**, *16*, 15839−15845.

(10) Fujiyama, S.; Kamiya, N.; Nishi, K.; Yokomori, Y. Reanalysis of CO2-silicalite-1 structure as monoclinic twinning. *Z. Kristallogr. - Cryst. Mater.* **2014**, *229*, 303−309.

(11) Fujiyama, S.; Kamiya, N.; Nishi, K.; Yokomori, Y. Location of CO2 on silicalite-1 zeolite using a single crystal x-ray method. *Z. Kristallogr. - Cryst. Mater.* **2013**, *228*, 180−186.

(12) Choudhary, V. R.; Mayadevi, S. Adsorption of methane, ethane, ethylene and carbon dioxide on silicalite-I. *Zeolites* **1996**, *17*, 501−507.

(13) Razavian, M.; Fatemi, S.; Masoudi-Nejad, M. A comparative study of CO2 and CH4 adsorption on silicalite-1 fabricated by sonication and conventional method. *Adsorpt. Sci. Technol.* **2014**, *32*, 73−87.

(14) Hirotani, A.; Mizukami, K.; Miura, R.; Takaba, H.; Miya, T.; Fahmi, A.; Stirling, A.; Kubo, M.; Miyamoto, A. Grand canonical Monte Carlo simulation of the adsorption of CO2 on silicalite and NaZSM-5. *Appl. Surf. Sci.* **1997**, *120*, 81−84.

(15) Babarao, R.; Hu, Z.; Jiang, J.; Chempath, S.; Sandler, S. I. Storage and separation of CO2 and CH4 in silicalite, C168 schwarzite and IRMOF-1: A comparative study from Monte Carlo simulation. *Langmuir* **2007**, *23*, 659−666.

(16) Santoro, M.; Gorelli, F.; Haines, J.; Cambon, O.; Levelut, C.; Garbarino, G. Silicon carbonate phase formed from carbon dioxide and silica under pressure. *Proc. Natl. Acad. Sci. U. S. A.* **2011**, *108*, 7689−7692.

(17) Santamaria-Perez, D.; McGuire, C.; et al. Strongly-driven Re +CO2 redox reaction at high-pressure and high-temperature. *Nat. Commun.* **2016**, *7*, 13647.

(18) Santamaria-Perez, D.; McGuire, C.; et al. Exploring the chemical reactivity between carbón dioxide and three transition metals (Au, Pt, and Re) at high pressures and temperatures. *Inorg. Chem.* **2016**, *55*, 10793−10799.

(19) Haines, J.; Levelut, C.; Isambert, A.; Hébert, P.; Kohara, S.; Keen, D. A.; Hammouda, T.; Andrault, D. Topologically ordered amorphous silica obtained from the collapsed siliceous zeolite, silicalite-1-F: A step toward "perfect" glasses. *J. Am. Chem. Soc.* **2009**, *131*, 12333−12338.

(20) Haines, J.; Cambon, O.; Levelut, C.; Santoro, M.; Gorelli, F.; Garbarino, G. Deactivation of pressure-induced amorphization in silicalite SiO2 by insertion of guest species. *J. Am. Chem. Soc.* **2010**, *132*, 8860−8861.

(21) Sartbaeva, A.; Haines, J.; Cambon, O.; Santoro, M.; Gorelli, F.; Levelut, C.; Garbarino, G.; Wells, S. A. Flexibility Windows and

DOI: 10.1021/acs.inorgchem.8b00523
Inorg. Chem. XXXX, XXX, XXX−XXX

compression of monoclinic and orthorhombic silicalites. *Phys. Rev. B: Condens. Matter Mater. Phys.* **2012**, *85*, 064109.
(22) Santamaria-Perez, D.; Marqueño, T.; MacLeod, S.; Ruiz-Fuertes, J.; Daisenberger, D.; Chulia-Jordan, R.; Errandonea, D.; Jorda, J. L.; Rey, F.; McGuire, C.; Mahkluf, A.; Kavner, A.; Popescu, C. Structural evolution of CO2-filled pure silica LTA zeolite under high-pressure high-temperature conditions. *Chem. Mater.* **2017**, *29*, 4502−4510.
(23) Palomino, M.; Corma, A.; Rey, F.; Valencia, S. New insights on CO2-methane separation using LTA zeolites with different Si/Al ratios and a first comparison with MOFs. *Langmuir* **2010**, *26*, 1910−1917.
(24) Guth, J.-L.; Kessler, C.; Wey, R. New Route to Pentasil-Type Zeolites Using a Non Alkaline Medium in the Presence of Fluoride Ions. *Stud. Surf. Sci. Catal.* **1986**, *28*, 121.
(25) Heitmann, G. P.; Dahlhoff, G.; Hölderich, W. F. Catalytically active sites for the Beckmann rearrangement of cyclohexanone oxime to epsilon-caprolactam. *J. Catal.* **1999**, *186*, 12−19.
(26) Dewaele, A.; Loubeyre, P.; Mezouar, M. Equations of State of Six Metals above 94 GPa. *Phys. Rev. B: Condens. Matter Mater. Phys.* **2004**, *70*, 094112.
(27) Liu, L.-G. Compression and phase behavior of solid CO2 to half a megabar. *Earth Planet. Sci. Lett.* **1984**, *71*, 104−110.
(28) Giordano, V. M.; Datchi, F.; Gorelli, F. A.; Bini, R. Equation of state and anharmonicity of carbón dioxide phase I up to 12 GPa and 800 K. *J. Chem. Phys.* **2010**, *133*, 144501.
(29) Dorogokupets, P. I.; Dewaele, A. Equations of state of MgO, Au, Pt, NaCl-B1, and NaCl-B2: Internally consistent high-temperature pressure scales. *High Pressure Res.* **2007**, *27*, 431−446.
(30) Fauth, F.; Peral, I.; Popescu, C.; Knapp, M. The new material science powder diffraction beamline at ALBA synchrotron. *Powder Diffr.* **2013**, *28*, s360−s370.
(31) Prescher, C.; Prakapenka, V. B. DIOPTAS: A Program for Reduction of Two-Dimensional X-Ray Diffraction Data and Data Exploration. *High Pressure Res.* **2015**, *35*, 223−230.
(32) Rodriguez-Carvajal, J. Recent Advances in Magnetic-Structure. *Phys. B* **1993**, *192*, 55−69.
(33) Nolze, G.; Kraus, W. Powdercell 2.0 for Windows. *Powder Diffraction* **1998**, *13*, 256−259.
(34) Laugier, J.; Bochu, B. *LMGP Suite of Programs for the Interpretation of X-ray Experiments*; ENSP/Laboratoire des Matériaux et du Génie Physique: France, http://www.inpg.fr/LMGP and http://www.ccp14.ac.uk/tutorial/lmgp.
(35) Santamaria-Perez, D.; Ruiz-Fuertes, J.; Marqueño, T.; Pellicer-Porres, J.; Chulia-Jordan, R.; MacLeod, S.; Popescu, C. Structural behavior of natural silicate-carbonate spurrite mineral, Ca5(SiO4)2-(CO3), under high-pressure, high-temperature conditions. *Inorg. Chem.* **2018**, *57*, 98−105.
(36) Hohenberg, P.; Kohn, W. Inhomogeneous Electron Gas. *Phys. Rev.* **1964**, *136*, B864−B871.
(37) Kresse, G.; Hafner. Ab initio molecular dynamics for liquid metals. *Phys. Rev. B: Condens. Matter Mater. Phys.* **1993**, *47*, 558; *Phys. Rev. B: Condens. Matter Mater. Phys.* **1994**, *49*, 14251.
(38) Kresse, G.; Furthmüller. Efficiency of ab-initio total energy calculations for metals and semiconductors using a plane-wave basis set. *Comput. Mater. Sci.* **1996**, *6*, 15.
(39) Kresse, G.; Furthmüller. Efficient iterative schemes for ab initio total-energy calculations using a plane-wave basis set. *Phys. Rev. B: Condens. Matter Mater. Phys.* **1996**, *54*, 11169.
(40) Blöchl, P. E. Projector Augmented-Wave Method. *Phys. Rev. B: Condens. Matter Mater. Phys.* **1994**, *50*, 17953−17979.
(41) Perdew, J. P.; Ruzsinszky, A.; Csonka, G. I.; Vydrov, O. A.; Scuseria, G. E.; Constantin, L. A.; Zhou, X.; Burke, K. Restoring the density-gradient expansion for exchange in solids and surfaces. *Phys. Rev. Lett.* **2008**, *100*, 136406.
(42) Perdew, J. P.; Burke, K.; Ernzerhof, M. Generalized gradient approximation made simple. *Phys. Rev. Lett.* **1996**, *77*, 3865.
(43) Grimme, S. Semiempirical GGA-type density functional constructed with a long-range dispersion correction. *J. Comput. Chem.* **2006**, *27*, 1787−1799.
(44) Grimme, S.; Antony, J.; Ehrlich, S.; Krieg, S. A consistent and accurate ab initio parametrization of density functional dispersion correction (DFT-D) for the 94 elements H − Pu. *J. Chem. Phys.* **2010**, *132*, 154104.
(45) Artioli, G.; Lamberti, C.; Marra, G. L. Neutron powder diffraction study of orthorhombic and monoclinic defective silicalite. *Acta Crystallogr., Sect. B: Struct. Sci.* **2000**, *56*, 2−10.
(46) Inui, M.; Ikeda, T.; Suzuki, T.; Sugita, K.; Mizukami, F. Quantitative analysis of structural defect in silicalite by Rietveld refinements using X-ray powder diffraction and (29)Si MAS NMR. *Bull. Chem. Soc. Jpn.* **2009**, *82*, 1160−1169.
(47) http://europe.iza-structure.org/IZA-SC/framework.php?STC=MFI.
(48) Fitch, A. N.; Jobic, H.; Renouprez, A. Location of benzene in sodium-Y zeolite by powder neutron diffraction. *J. Phys. Chem.* **1986**, *90*, 1311−1318.
(49) Birch, F. Finite elastic strain of cubic crystals. *Phys. Rev.* **1947**, *71*, 809.
(50) Richard, J.; Cid, S. L.; Rouquette, J.; Van der Lee, A.; Bernard, S.; Haines, J. Pressure-induced Insertion of ammonia borane in the siliceous zeolite, silicalite-1F. *J. Phys. Chem. C* **2016**, *120*, 9334−9340.
(51) Qu, B.; Li, D.; Wang, L.; Zhou, R.; Zhang, B.; Zeng, X.-C.; Wu, J. Mechanistic study of pressure and temperature dependent structural Changes in reactive formation of silicon carbonate. *RSC Adv.* **2016**, *6*, 26650−26657.
(52) Pabst, W.; Gregorova, E. Elastic properties of silica polymorphs − A review. *Ceramics* **2013**, *57*, 167−184.
(53) Quartz is found to exist in a distorted form (to be published).
(54) Akaogi, M.; Yusa, H.; Shiraishi, K.; Suzuki, T. Thermodynamic properties of α-quartz, coesite and stishovite and equilibrium phase relations at high pressures and high temperatures. *J. Geophys. Res.* **1995**, *100*, 22337−22347.
(55) Gatta, G. D. Does porous mean soft? On the elastic behaviour and structural evolution of zeolites under pressure. *Z. Kristallogr. - Cryst. Mater.* **2008**, *223*, 160−170.
(56) Gatta, G. D. Extreme deformation mechanisms in open-framework silicates at high-pressure: Evidence of anomalous inter-tetrahedral angles. *Microporous Mesoporous Mater.* **2010**, *128*, 78−84.
(57) Gatta, G. D.; Lotti, P.; Tabacchi, G. The effect of pressure on open-framework silicates: elastic behaviour and crystal−fluid interaction. *Phys. Chem. Miner.* **2018**, *45*, 115−138.

DOI: 10.1021/acs.inorgchem.8b00523
Inorg. Chem. XXXX, XXX, XXX−XXX